A review of critical scouring velocity of compact roof aggregate

Doddipatla, L.S.; Kopp, Gregory

[Link to publication on Research at Birmingham portal](#)

A Review of Critical Scouring Velocity of Compact Roof Aggregate

Lakshmana S. Doddipatla[a], Gregory A. Kopp[b]

[a]*FM Global, Research Division, Norwood, MA, USA, lakshmana.doddipatla@fmglobal.com*

[b]*Boundary Layer Wind Tunnel Laboratory, Faculty of Engineering, University of Western Ontario, London, ON, Canada., gakopp@uwo.ca*

ABSTRACT:

This paper provides a review of previous studies on how various building parameters affect the critical scouring velocity of roof aggregate, and how these data can be used from a risk mitigation point of view. The review suggests that the data are available only up to a building height of 45 m, with and without parapets, and with no roof-mounted equipment. However, loosely-laid roof aggregate is currently used up to an approximate building height of 150 m in some cities, and these buildings usually have substantial roof-mounted equipment and parapets that are typically less than 1.8 m high. The available data may not necessarily provide reliable recommendations when extrapolated to these high-rise buildings as the aerodynamics of low-rise to high-rise buildings are different and can be influenced by the presence of roof-mounted equipment. The paper concludes by suggesting confidence limits when extrapolating existing data and identifying areas that need further research to address the critical scouring velocity of loosely-laid roof aggregate for low-rise and high-rise buildings.

KEYWORDS: Wind-borne debris; loosely-laid roof aggregate; critical scouring velocity; building aerodynamics; wind loads.

1. INTRODUCTION

Extensive evaluation by Minor (1994) and Kareem and Bashor (2006) after significant hurricane events demonstrated that wind-borne debris is one of the primary causes of building envelope damage. Wind-borne debris arises from a variety of sources including building components such as tiles, shingles, metal sheeting, timber structural members of low-rise buildings, and loosely-laid roof aggregate such as roof gravel on built-up roofs (BUR) (Owen, 2015, Holmes, 2010, Kaye, 2017). Wills et al. (2002) classified wind-borne debris into three generic types: (a) compact, (b) rod, and (c) sheet. Debris, when picked up by the wind, can accelerate and travel long distances, and gain significant momentum before reaching the ground or downstream buildings. Typical damage includes broken windows and penetration of the building envelope. It is important to note that, once the envelope of the building is breached, internal

31   pressurization of the building can cause progressive failure of various building components, leading to

32   extensive damage and additional wind-borne debris, which can further impact surrounding buildings.

33   Hence, wind-borne debris poses a significant hazard and, thus, arises the necessity to understand this

34   hazard and the influencing parameters to develop risk mitigation solutions.

35   Crushed stone or gravel used as roof ballast that can be classified as the compact type is of interest in this

36   review and will be the only type that will be explored further. Karimpour and Kaye (2012) provide a clear

37   and succinct review of the interaction of loose particles with fluid flow in the context of sediment

38   transport and wind erosion based on the work by Shields (1936) and Bagnold (1937), respectively.

39   Shields (1936) proposed that critical shear stress for sediment transport in non-dimensional form can be

40   written as

$$\frac{\tau_c}{(\rho_p - \rho_f)gd} = \frac{\rho_f u_{*c}^2}{(\rho_p - \rho_f)gd} = \frac{u_{*c}^2}{((\rho_p - \rho_f)/\rho_f)gd} = Fr_*^2 \tag{1}$$

41   where τ_c is the critical shear stress, ρ_p is the density of the particle, ρ_f is the density of the fluid, d is the

42   particle diameter, u_{*c} is the friction velocity, and g is the acceleration due to gravity. The left-hand side

43   of the equation is also called the critical Shields parameter, which is the square of the densimetric Froude

44   number (Fr_*). Karimpour and Kaye (2012) suggest that the underlying physics of sediment transport and

45   wind erosion is similar to that of the wind-borne debris of roof aggregate since, in both cases, the fluid is

46   interacting with loosely-laid particles. They indicated that the Froude number is dependent on

$$Fr_d^2 = f\left(Re_d, \frac{H}{h}, \frac{H}{w}\right) \tag{2}$$

47   where H is the parapet height, h is the building height, w is the width of the building. The Reynolds

48   number (Re_d) and Froude number (Fr_d) are calculated using the wind velocity at the top of the parapet (

49   U_H) instead of the friction velocity (u_{*c}) used in Eq. (1). According to Karimpour and Kaye (2012,

50   2013), the roof gravel blow-off failure mechanism can be envisioned as a three-part problem:

51   1. Motion initiation – This is the process through which aggregate is lifted from the roof, out of the cavity

52   formed by the parapets. This part of the problem identifies the building parameters that will affect the

53   roof height velocity, which in turn governs the motion initiation of the roof gravel.

54   2. Removal – This is the stage that relates the motion initiation and quantifies the aggregate removal rate

55   from the roof. This part of the problem identifies the downwind risk of debris impact.

56 3. Flight – This stage quantifies the distance the aggregate travels in the downstream direction before

57   impact. This part of the problem identifies the parameters that will affect how far the gravel can travel

58   once it becomes airborne.

59 *Motion initiation* of wind-borne debris relates to the critical scouring velocity of roof aggregate, which is

60 the primary focus of this review paper. Hence, *removal* and *flight* of wind-borne debris are not discussed

61 here. This paper reviews model-scale wind tunnel experiments that were conducted by Kind (1973, 1974,

62 1975), Kind and Wardlaw (1976, 1977, 1985), and Kind et al. (1984, 1987) at the National Research

63 Council (NRC) of Canada, Kind (1986) at Carleton University, Phalen Jr. (1984, 1985) at Northeastern

64 University, Karimpour and Kaye (2012, 2013) at Clemson University, and by Kopp (2009) at the

65 University of Western Ontario with the objective to collate all the available experimental data in order to:

66   • Understand the relationship between Reynolds and Froude number,

67   • Develop guidelines for risk mitigation for different classes of buildings, i.e., low- and high-rise,

68   and

69   • Identify areas that need further research.

70 The following sections describe the details of these experimental studies along with a summary of

71 experimental data, followed by a comparison of critical scouring velocity among all studies. Some

72 conclusions are drawn, and guidelines are presented along with assumptions that identify areas for future

73 research.

74 **2. SUMMARY AND ANALYSIS OF PREVIOUS RESEARCH**

75 **2.1 Data from NRC Canada**

76 This section summarizes the work done at the National Research Council (NRC) of Canada by Kind and

77 his coworkers. The work has been summarized in publications by Kind (1973, 1974, 1975), Kind and

78 Wardlaw (1976, 1977, 1985), and Kind et al. (1984, 1987). These studies address critical scouring

79 velocities of loosely-laid roof aggregate as a function of building height, parapet height, gravel size, along

80 with the effects of building corners covered with paver blocks instead of roof gravel.

81 *2.1.1 Experimental Setup*

82 All the dimensions including gravel sizes and parapet heights were tested at a model scale of 1:10. Three

83 identical building blocks with equivalent full-scale dimensions (Length x Width x Height) of 22.9 x 4.6 x

84 4.6 m were constructed and used in combinations to model various building heights and plan dimensions

85 for low-rise building (Kind, 1973). Another low-rise building size that was also tested was 13.7 x 13.7 x

86 2.7 m. Two high-rise building sizes (i.e., buildings that are taller than wide) were tested corresponding to

87   9.1 x 9.1 x 22.9 m and 18.3 x 9.1 x 22.9 m. Various parapet heights were tested ranging from 0.06 m to

88   1.37 m. Three different gravel sizes corresponding to 22.9 mm, 38.1 mm, and 72.1 mm (in equivalent

89   full-scale) were tested, with the gravel spread to depths of about 63.5 mm, 76.2 mm, and 127 mm.

90   Additional experiments also consisted of including paving blocks in the corner of the roof, which is

91   defined by the parameters a and b as shown in Fig. 1. (The paving blocks were included to understand

92   how the scouring velocity changes with the influence of corner vortices.) However, little information

93   regarding the turbulence characteristics or turbulence spectra of terrain simulation is provided, except for

94   the reported gust factors for different building heights, which are summarized in Table 1.

95   ### *2.1.2 Experimental Data*

96   Table 2 summarizes the equivalent full-scale experimental data from Kind's experiments. Kind (1975)

97   identified four different wind speeds (U_{C1}, U_{C2}, U_{C3}, and U_{C4}) defined as: (i) U_{C1} is the wind speed at

98   which one or more stones are first observed to move an appreciable distance. No gravel will leave the

99   roof at this wind speed; (ii) U_{C2} is the wind speed above which scouring of stones would continue more or

100   less indefinitely as long as the wind speed is maintained. No gravel will leave the roof at this wind speed;

101   (iii) U_{C3} is the wind speed at which few stones are observed to leave the roof by going over the upstream

102   parapet (AB in Fig. 1); (iv) U_{C4} is the wind speed at which a few stones are observed to leave the roof by

103   going over the downstream parapet (BC in Fig. 1). The four different wind speeds summarized in Table 2

104   are 1-s gust wind speeds at roof height. These values are obtained by multiplying the mean hourly wind

105   speeds at the 9.1 m above the ground with their respective gust factors corresponding to building heights

106   summarized in Table 1.

107   Kind and Wardlaw (1976) noted that the motion of the stones lasts for a limited time when subjected to

108   wind speeds between U_{C1} and U_{C2}. The stones start to scour continuously when wind speed is greater than

109   or equal to U_{C2}. The uncertainty in the wind speed around U_{C2} is about 10% as it is difficult to identify

110   constant scouring during the experiments. The uncertainty around U_{C3} and U_{C4} is around 20 % as a small

111   number of stones could leave the roof at lower wind speeds than those noted in Table 2. Little information

112   is provided as to how these uncertainties were calculated by Kind and Wardlaw (1976). Based on the

113   description of different critical velocities, U_{C2} is the critical scour velocity that is of importance in this

114   study as this speed relates to the wind speed just before failure of the gravel and will be analyzed further

115   in the following discussion.

116   ### *2.1.3 Building Classification*

117   Kind and Wardlaw (1976) classify a building as low-rise when

$$2.5(h + 3H) \leq l \text{ and } 2.5(h + 3H) \leq w \tag{3}$$

118 where h is the height of the building, H is the height of the parapet, l is the length of the building, and w

119 is the width of the building. Even though Kind and Wardlaw (1976) did not provide any justification for

120 Eq.(3), the possible intent would have been to identify the limiting case of the low-rise building that is

121 strongly influenced by the corner vortices. SEAOC-PV2 (2017) uses a similar equation, i.e., wall aspect

122 ratio ($l/h \text{ or } w/h \leq 2.5$) to limit the effect of corner vortices, as the corner vortices do not get much

123 stronger for larger wall aspect ratios. However, based on the data presented in Table 2, Eq. (3) does not

124 classify building heights of 9.1 m and 13.7 m as low-rise even though the height is less than the least

125 horizontal dimension. Therefore, a new building classification is proposed for low- to mid-rise building as

$$2.5(h + 3H) > l, \; 2.5(h + 3H) > w, \; h < l, \text{ and } h < w \tag{4}$$

126 which accounts for building heights of 9.1 m and 13.7 m. Buildings which satisfy equation (4) are termed

127 as low- to mid-rise herein. Kind and Wardlaw (1976) classifies a building as high-rise when

$$h \geq (l + w) \tag{5}$$

128 However, based on the data presented in Table 2, Eq.(5) only classifies buildings with dimensions 9.1 x

129 9.1 x 22.9 m as high-rise. Buildings with dimensions 9.1 x 18.2 x 22.9 m do not agree with Eq. (5).

130 Therefore, a new high-rise building classification is proposed as

$$h < (l + w), \; h > l, \text{ and } h > w \tag{6}$$

131 which leads to the building with dimensions 9.1 x 18.2 x 22.9 m being classified as another class of high-

132 rise. Equation (5) is termed as high-rise I and Eq. (6) is termed as high-rise II, herein.

2.1.4 Assumptions

134 Kind (1975) assumed that the same 1-s gust wind speeds in Table 2 at the rooftop level would cause

135 failure of roof gravel for geometrically similar buildings of different heights for a particular gravel size.

136 Based on the building classifications presented in Section 2.1.3, this assumption implies that, as long as

137 the ratios l/h and w/h fall within a range, the different critical velocities presented in Table 2 can be

138 assumed to be independent of the building height. Akon (2017) suggested that roof height wind speed is

139 constant only when the ratios of l/h and w/h, and the longitudinal turbulence intensity at the building

140 height are the same based on a study of the different size of low-rise buildings. Hence, it can be

141 concluded that Kind's (1975) assumption is reasonable, considering that it is a modest relaxation of

142   criteria suggested by Akon (2017), which allows one to generalize the results from the available

143   experimental data.

2.1.5 Critical Scouring Velocity

145   In order to account for various building parameters and the gravel sizes that influence the critical scouring

146   velocity, Kind and Wardlaw (1976) define the critical scouring velocity as being dependent on the three

147   variables in the following expression

$$U_{c2} = (F_S)(F_P)(U_{C_{ref}}) \tag{7}$$

148   where

149   F_S = gravel size factor that accounts for the size of the gravel;

150   F_P = parapet height/paving block array factor that accounts for the parapet height and paving block

151   dimensions;

152        $U_{C_{ref}}$ = Reference critical wind speed that is assumed to be constant for each class of building.

153   These variables will be discussed in the following sections.

2.1.6 Gravel Size Factor (F_S)

155   Kind and Wardlaw (1976) use Froude scaling to convert model-scale data to full scale with the

156   assumption that the Froude number is constant and independent of the Reynolds number. This assumption

157   implies that the scouring velocity at full scale can be obtained from model-scale experiments using

158   (Karimpour and Kaye, 2012)

$$U_{FS} = U_{MS}\sqrt{\frac{d_{FS}}{d_{MS}}} \tag{8}$$

159   where the subscript FS indicates full scale and MS indicates model scale, while d is the particle diameter.

160   Kind and Wardlaw (1976) termed the ratio $\sqrt{d_{FS}/d_{MS}}$ as the gravel size factor (F_S), and suggested that

161   Eq. (8) can also be used to scale the experimental data for different gravel sizes, when the critical

162   scouring velocity is known for a particular gravel size as

$$U_{required\ gravel\ size} = U_{known\ gravel\ size}\sqrt{\frac{d_{required\ gravel\ size}}{d_{known\ gravel\ size}}} \tag{9}$$

163   Equation (9) is plotted in Fig. 2, where Kind and Wardlaw (1976) used 19.1 mm as the reference (or

164   known) gravel size and presented F_S for the critical scouring velocity that can be calculated for other

165   gravel sizes.

2.1.7 Parapet Height/Paving Block Array Factor (F_P)

167   Kind and Wardlaw (1976) present parapet height/paving block array factors (F_P) (see Fig. 3) that account

168   for the parapet height and paving block dimensions for (a) low-rise, (b) high-rise I, and (c) high-rise II

169   buildings. As the interdependence of the building shape, parapet height, and paving block array cannot be

170   individually quantified, Kind and Wardlaw (1976) defines the factor F_p as the ratio

$$F_p = \frac{U_{C(d)}}{U_{C_{ref}}} \tag{10}$$

171   where $U_{C(d)}$ is the roof height critical velocity for a particular gravel size (d) and $U_{C_{ref}}$ is an arbitrarily

172   chosen reference critical wind speed (see Section 2.1.8).

173   Kind and Wardlaw (1976) present the parapet height/paving block array factors (F_P) as a function of the

174   parapet height (H) divided by the building height (h) for a low-rise building ($h \ll l,w$), and by the

175   building width (w) for a high-rise building ($h \gg l,w$), to take advantage of the universality of the data

176   regardless of the actual height, length and width of the building. Not many details are provided in the

177   report by Kind and Wardlaw (1976) on how F_P was obtained except for Eq. (10). They present factors

178    $F_{p\,1,2}$ (see Fig. 3) used to calculate U_{c1} and U_{c2}, and $F_{p\,3}$ (not shown), to calculate U_{c3}. Kind and

179   Wardlaw (1976) noted that, in the case of U_{c4}, since the stones must travel the whole roof length to leave

180   the rooftop from the downstream parapet, the speed of the stone cannot be assumed to be negligible

181   compared to the speed of the airflow. Hence, the analysis used for velocities U_{c1}, U_{c2}, and U_{c3} cannot be

182   used for U_{c4} to make generalized recommendations. Therefore, Kind and Wardlaw (1976) did not provide

183   any recommendations for U_{c4}.

2.1.8 Reference Critical Wind Speed $\left(U_{C_{ref}}\right)$

185   Kind and Wardlaw (1976) recommend using a reference critical wind speed $\left(U_{C_{ref}}\right)$ of 35.3 m/s, 34.4 m/s,

186   and 29.9 m/s to estimate the critical scouring velocity (U_{C2}) when the gravel size is 19.1 mm (i.e., $F_S = 1$)

187   for low-rise and the two types of high-rise buildings, respectively. Kind and Wardlaw (1976) arbitrarily

188   chose these scouring wind speeds for a particular case with the intent to obtain scouring wind speeds by

189   multiplying the reference critical wind speed $\left(U_{C_{ref}}\right)$ with appropriate factors to account for the different

190   gravel sizes (F_S), parapet height and paving block geometry (F_P). However, it can be noted from Table 2,

7

191   that Kind (1975) did not perform experiments for a gravel size of 19.1 mm, and Kind and Wardlaw

192   (1976) did not provide any explanation for how $U_{C_{ref}}$ was estimated for this gravel size.

2.1.9 Further Analysis of NRC Data

194   In the following section, the experimental data summarized in Table 2 will be analyzed to understand the

195   basis for the parapet height/paving block array factor (F_P) and the reference critical wind speed $\left(U_{C_{ref}}\right)$

196   proposed by Kind and Wardlaw (1976) for a 19.1 mm gravel size.

2.1.9.1   Low-rise Building

198   From Fig. 3 (a) it can be noted that Kind and Wardlaw (1976) normalized their experimental data by

199   dividing the velocity at $H/h = 0.1$ for $a = 0$ and $b = 0$, where a and b are defined in Fig. 1. For a low-rise

200   building, data (see Table 2) are available for three gravel sizes corresponding to 22.9 mm, 38.1 mm, and

201   72.1 mm. The corresponding critical scouring velocities of 38.0 m/s, 44.3 m/s, and 55.0 m/s at $H/h = 0.1$

202   for $a = 0$, and $b = 0$ are used as reference critical wind speeds $\left(U_{C_{ref}}\right)$ in Eq. (10) to obtain the parapet

203   height/paving block array factor (F_P). It can be noted from Table 2 that, for the same H/h ratios, multiple

204   values are available from different experiments, in which case the minimum velocity from all available

205   experiments is taken as the reference critical wind speed. The parapet height/paving block array factors (

206   F_P) are plotted in Fig. 4 for different gravel sizes and different paver block dimensions. It can be noted

207   from the comparison that the Kind and Wardlaw (1976) proposed $F_{p\,1,2}$ curves compare well with the

208   experimental data. However, there are few data points ($a = 0.25\,h$, $b = 0.25\,h$, $a = 0.5\,h$, $b = 1.0$

209   h, and $a = 1.0\,h$, $b = 2.0\,h$) that suggest that the corresponding $F_{P_{1,2}}$curves were based partially on

210   judgment since no functional form based on mechanics is provided.

211   The next question that needs to be addressed is the basis for the reference critical wind speed ($U_{C_{ref}}$) of

212   35.3 m/s proposed by Kind and Wardlaw (1976) for a gravel size of 19.1 mm. Figure 5 plots the critical

213   scouring wind speed for different gravel sizes. The reference critical wind speed ($U_{C_{ref}}$) corresponding to

214   a gravel size of 19.1 mm is assumed to be obtained by linearly extrapolating the data, which yields a

215   value of 36.4 m/s. Comparing reference critical wind speeds of 35.3 m/s and 36.4 m/s, it can be noted that

216   the difference of the Kind and Wardlaw (1976) recommended reference critical wind speed is

217   approximately 3%, which is within the estimated uncertainty of 10% for the experimental data. Hence, it

218   can be stated that the reference critical wind speed proposed by Kind and Wardlaw (1976) to be used with

219   the Parapet Height/Paving Block Array Factors (F_P) agree reasonably well with the experimental data

220   presented in Table 2.

221   Since the critical scouring wind speeds for different gravel sizes are available from experimental data,

222   Eq.(9) can be verified. The critical scouring velocities for different gravel sizes (i.e., 22.9 mm, 38.1 mm,

8

223   and 72.1 mm) can be calculated using Eq.(9) with a reference critical wind speed $(U_{C_{ref}} = 35.3$ m/s)

224   proposed by Kind and Wardlaw (1976) for a gravel size of 19.1 mm. This is shown as the dashed line in

225   Fig. 6 compared with experimental data shown by the solid line. It can be noted that the critical scouring

226   velocities suggested by Kind and Wardlaw (1976) for different gravel sizes are higher compared to what

227   is obtained from the experimental data. These higher critical scouring velocities imply that the gravel can

228   sustain higher wind speeds before they start to scour, when compared to what the experimental data

229   suggest. The difference in the velocities noted in Fig. 6 is much higher for larger gravel sizes. Therefore,

230   it can be concluded that the gravel size factor (Eq.(9)) proposed by Kind and Wardlaw (1976) based on

231   the assumption that Froude number is constant and independent of Reynolds number is not completely

232   accurate and needs to be investigated further.

233   *2.1.9.2   High-Rise Building I and High-Rise Building II*

234   From Fig. 3 (b and c) it can be noted that Kind and Wardlaw (1976) normalized their experimental data

235   by dividing the critical velocity at $H/w = 0.025$ for $a = 0$ and $b = 0$ instead of $H/h = 0.1$, $a= 0$, and $b=0$

236   for a low-rise building. An analysis similar to that for the low-rise buildings (see Section 2.1.9.1) is

237   performed for the high-rise buildings from Table 2, and hence the details of the analysis are not presented

238   here. The comparison (Fig. 7 and Fig. 9) indicates that the data agree with the Parapet Height/Paving

239   Block Array Factor (F_P), but there are limited data when compared to those for the low-rise buildings.

240   These scouring velocity comparisons (Fig. 8 and Fig. 10) indicate that Kind and Wardlaw (1976)

241   recommend higher critical velocities for roof gravel failure than the experimental data, especially for

242   gravel sizes greater than 38.1 mm.

243   *2.1.9.3   Revised Gravel Size Factor*

244   In order to correct the critical velocities obtained based on Kind and Wardlaw (1976) recommendations, a

245   velocity correction factor is proposed that is obtained by dividing the actual scouring velocities from the

246   experiments with the scouring velocities obtained from Kind and Wardlaw (1976) recommendations.

247   These are plotted in Fig. 11 for low-rise buildings. Similar correction factors can be obtained for high-rise

248   building I and high-rise building II. These velocity correction factors can be combined with the gravel

249   size factor (F_S) discussed in Section 2.1.5, and a revised gravel size factor can be obtained as shown in

250   Fig. 12.

251   Based on the curves presented in Fig. 12, it can be noted that the revised gravel size factor for the low-rise

252   building deviates the most from what is recommended by Kind and Wardlaw (1976) especially for gravel

253   sizes greater than 25 mm. On the other hand, the revised gravel size factor for high-rise I appears to be the

254   closest match with what is recommended by Kind and Wardlaw (1976), even though it deviates

255 substantially for gravel sizes greater than 35 mm. The revised gravel size factor for high-rise II varies

256 between that of low-rise and high-rise I, depending on the gravel size.

2.2 Data from Carleton University

258 The section summarizes the measurements from Kind (1986) at Carleton University at a model scale of

259 1:60 and 1:120 for five model-scale gravel sizes ranging from 0.2 mm to 0.72 mm equivalent to a full-

260 scale gravel size ranging from 21 mm to 43.2 mm. Table 3 summarizes the critical scouring velocity (U_{c2})

261 results from these experiments.

2.2.1 *Experimental Setup*

263 Kind (1986) retested the 1:10 (Kind, 1975) model-scale experiments at smaller scales of 1:60 and 1:120

264 to investigate the effect of Reynolds number. The experiments were carried out in the Carleton University

265 wind tunnel having dimensions of 1.2 m high x 1.7 m wide x 12 m long. Natural silica was used to model

266 the gravel size corresponding to five model-scale sizes of 0.2 mm, 0.35 mm, 0.51 mm, 0.63 mm, and 0.72

267 mm.

2.2.2 *Experimental Data*

269 The critical velocities U_{C1}, U_{C2}, and U_{C3} were measured similar to those in Kind's 1:10 scale experiments

270 (Kind, 1975); however, only data for U_{C2} were presented in the publication (Kind, 1986). Figure 13(a)

271 shows the comparison of model-scale critical scouring wind speeds at 1:60 and 1:120 scales (Kind, 1986)

272 compared with 1:10 model-scale experiments (Kind and Wardlaw, 1976) for a low-rise building. It should

273 be noted that the data presented in Fig. 13(a) are model-scale data, whereas the 1:10 model-scale data

274 from Kind and Wardlaw (1976) were used for a gravel size of 19.1 mm. Based on these comparisons,

275 Kind (1986) noted that the model-scale data are subjected to Reynolds number effects and proposed a

276 correction factor. However, Kind (1986) did not present how the corrected data would compare with their

277 1:10 model-scale experiments. Karimpour and Kaye (2012) presented the corrected data (presented in

278 Fig. 13 (b)) and concluded that the corrected data are approximately 30 % lower than the 1:10 model-

279 scale data from Kind and Wardlaw (1976). They suggest that the correction method proposed by (Kind,

280 1986) does not completely eliminate the Reynolds number effects and conclude by stating that the

281 Reynolds number effects can only be fully addressed by conducting full-scale experiments.

2.2.3 *Further Analysis of Carleton University Data*

283 The data presented in Fig. 13 are comparing the Kind and Wardlaw (1976) 1:10 model-scale data for a

284 full-scale gravel size of 19.1 mm with Kind's (1986) 1:60 and 1:120 model-scale data for different gravel

285 sizes. This comparison of data at different model scales is not appropriate because it violates the Froude

286 scaling relationship. Hence, Fig. 14 presents the comparison of Kind and Wardlaw (1976) and Kind's

287 (1986) model-scale data converted to full-scale using the Froude Scaling relationship presented in Eq. (8).

288 Kind and Wardlaw (1976) data for different gravel sizes were estimated using the revised gravel size

289 factors presented in Fig. 12.

290 Based on the comparisons of critical scouring velocity (U_{C2}) at different gravel sizes in Fig. 14, it can be

291 noted that the 1:60 model scale compares reasonably well with 1:10 model-scale data, whereas the 1:120

292 model scale predicts scouring velocities that are much higher than those from the 1:10 model-scale data.

293 Another interesting observation is that the large gravel size at 1:120 model scale has a relatively smaller

294 difference in U_{C2} compared to 1:10 model-scale data for smaller gravel sizes, suggesting that the physical

295 gravel sizes used in the model-scale experiments have an influence on U_{C2}. These comparisons contradict

296 the argument by Kind (1986) that aerodynamic drag on ballast stones is higher in small-scale tests

297 compared to full-scale, predicting lower full-scale critical scouring wind speeds when calculated based on

298 data obtained from model-scale experiments. However, the possible reasons for this trend are not clear. It

299 can be stated that uncertainty in experiments is higher when smaller model scales are used to obtain

300 critical scouring velocities. However, the correction factor proposed by Kind (1986) to account for

301 Reynolds number effects may not be appropriate and needs further research.

302 **2.3 Data from Northeastern University**

303 This section provides a summary of the work done by Phalen (1984, 1985) and Phalen and Smith (1984)

304 on the mechanics of gravel instability, scour, and movement under wind conditions for single-ply loosely-

305 laid roof membranes. Phalen (1984) conducted full-scale experiments to explain the scour mechanism of

306 stone ballast on a single-ply loosely-laid membrane. Figure 15 shows the experimental setup, which

307 consists of a cube-shaped building. The full-scale platform measured 3 x 3.6 m. However, information

308 about the building height is not reported. Parapets ranging from 0 to 0.9 m in increments of 0.15 m were

309 tested. The free-stream wind was developed from a 250 HP Continental 7-cylinder radial engine that was

310 connected to a 1.8 m propeller drive. Wind speeds in the range of 20.1 to 55.9 m/s were achieved during

311 the experiments. The geometry of the fans and the test structure was developed by trial and error to attain

312 an airstream 3.7 m wide and about 1.2 m thick when impinging on the structure. An observation platform

313 was used for photography during the experiments.

314 The test platform consisted of a single-ply Ethylene Propylene Diene Monomer (EPDM) membrane

315 loosely-laid on a structural deck. The membrane was sealed entirely along the edges by a flashing system

316 such that the roof system was airtight. The test measurements were provided by 22 Pitot tubes. In

317 addition, four monitors were used to measure wind speed on the roof. The direction of the wind that

318 impinged on the platform corresponded to 45°, which represented the severest condition based on the

319 work done by Kind and Wardlaw (1976). For each wind speed, the surface pressure was recorded at the

320   manometer locations. Phalen (1984) noted that each probe yielded a constant coefficient of pressure and

321   suggested using Bernoulli's equation in formulating a mathematical procedure to estimate scouring

322   velocity based on surface pressure variation on the roof as a function of parapet height.

2.3.1 Test Observations

324   Phalen (1984) observed that, when the wind interacted with the roof membrane, the pressure differential

325   had the effect to make the membrane expand upwards and caused the membrane to flutter, vibrate, and

326   oscillate, which cannot be simulated in model-scale experiments as rigid model-scale buildings are used.

2.3.2 Gravel Scour Wind Speed

328   Phalen (1984) measured the wind speed at which scour occurs. Table 5 summarizes the critical scouring

329   velocity (U_{c2}) from these experiments and Figure 16 shows the comparison of wind speed as a function of

330   stone diameter between Phalen (1984) and Kind and Wardlaw (1976) for a low-rise building. In spite of

331   the differences in the experimental approaches, the comparison indicates that Phalen's (1984) wind

332   speeds match those from Kind and Wardlaw (1976).

2.3.3 Differential Pressure

334   Phalen (1984) measured the differential pressure at the rooftop level during the experiments. He

335   developed a theoretical model to connect the differential pressure on the roof with the gravel resistance

336   for the case when the stone becomes wind-borne. The underlying assumption for this theoretical model is

337   that roof pressure coefficients are constant, and that the Bernoulli's equation can be used to adjust the

338   velocity based on the constant surface pressure coefficients. It should be noted that the surface pressure

339   coefficient on the roof is not constant and changes with time because of the separation reattachment and

340   corner vortices, while cause Bernoulli's equation not to hold near a roof surface (Wu et al., 2017). Phalen

341   (1984) reported a constant pressure coefficient as the measurements were performed using manometers

342   which will only measure mean values when tested for a particular wind direction, which is 45^0, in this

343   case. Hence, the analysis is not presented here as the mathematical model provided by Phalen (1984) is

344   not appropriate and is not explored further.

2.4 Data from Clemson University

346   This section summarizes the work conducted at Clemson University by Karimpour (2011) on a 1:20

347   model-scale building corresponding to full-scale building heights of 3.0, 4.0 and 6.0 m for different

348   parapet heights (0, 0.05, 0.1, 0.3, and 0.5 m), gravel sizes (2.2, 4.6, 7.2, 9.0, 10.2, 14.6, 17.8, 30.9, and 69

349   mm), and two different particle types (sand and millet). The width of the building spans the whole cross

350   section of the wind tunnel (3 m wide by 2 m high and 28 m long) with small clearances at the end to

351   represent a two-dimensional building. The experiments were conducted to capture the effect of

352   separating-reattaching flows. Karimpour and Kaye (2012) concluded that the Froude number can be

353   described using the relation for zero parapet heights as

$$\text{Fr}_d^2 = 8.1(d_*)^{-0.44} \tag{11}$$

354   where the non-dimensional particle diameter (d_*) is defined as

$$d_* = \left(\frac{Re_d}{Fr_d}\right)^{\frac{2}{3}} \tag{12}$$

355   The data had more spread when plotted for different parapet heights. However, Karimpour and Kaye

356   (2012) noted that zero parapet height data are not always the worst-case scenario, pointing out that their

357   results follow the observations made for roof pavers blow-off studies (Meroney and Bienkiewicz, 1986).

358   Based on these experiments, Karimpour and Kaye (2012) suggested that Reynolds number is a function of

359   Froude number for particle sizes up to $d_* = 75$ with no parapet. The data from this study were not used in

360   comparison with other studies as other experiments were mainly focused on an oblique wind angle of 45^0,

361   which captures the effect of corner vortices, instead of the perpendicular wind direction of 0^0 that was

362   used in this study, which captures the effects of separating-reattaching flow.

363   **2.5 Data from the University of Western Ontario**

364   The section summarizes the work conducted at the University of Western Ontario by Kopp (2009) on a

365   1:20 model-scale building with full-scale dimensions of 12.1 x 12.1 x 7.3 m for average gravel sizes of 30

366   mm and 43 mm. The experiments were conducted with and without surrounding buildings. The

367   experiments measured critical scour velocity as a function of wind direction (0^0, 30^0 and 45^0) and parapet

368   height (0.1 m, 0.3 m, 0.9 m, 1.8 m, and 2.7 m at full scale), and also measured the maximum height

369   attained by wind-borne gravels. Table 5 summarizes the critical scouring velocity (U_{c2}) from these

370   experiments. The building is classified as a low- to mid-rise based on the definitions presented in Section

371   2.1.3.

372   As the 45^0 building orientation governs the critical scouring velocity (Kind and Wardlaw, 1976), Fig. 17

373   compares the data from Kind (1975) and Kopp (2009) that are not in accordance with Eq.(4). The data

374   from Table 2 are used to obtain the mean wind speeds at roof height. As the data from Kind (1975) are for

375   a gravel size of 38 mm and these experiments are for a gravel size of 30 mm, Kind (1975) data were

376   adjusted using the revised gravel size factors summarized in Section 2.1.9.3 assuming that the buildings

377   can still be classified as low-rise buildings. The data fit provided in Fig. 17 for a gravel size of 30 mm is

378   expressed as

$$U_{C2} = 112.4\left(\frac{H}{h}\right) + 28.3 \text{ (m/s)} \tag{13}$$

379   Equation (13) can be converted to a gravel size of 19.1 mm, which is the reference gravel size used by

380   Kind and Wardlaw (1976), with the revised gravel size factors summarized in Section 2.1.9.3. Equation

381   (14) is obtained by multiplying Eq. (13) by a factor of 0.83 using equations summarized in Table 7 for the

382   low-rise building.

$$U_{C2} = 93.3\left(\frac{H}{h}\right) + 23.5 \text{ (m/s)} \tag{14}$$

383   The mean hourly wind speed obtained by Eq. (14) is converted to 3-seconds gust wind speed by

384   multiplying by a factor of 1.53 using the Durst (1924) curve, shown in Eq. (15)

$$U_{C2} = 142.7\left(\frac{H}{h}\right) + 35.9 \text{(m/s)} \tag{15}$$

385   ## 2.6 Discussion

386   The above sections have presented the experimental data from various studies that provide an estimate for

387   the critical scouring velocity. Even though the data from different studies were obtained at different

388   model scales, they were converted to full scale using the Froude scaling relationship along with the

389   revised gravel size factors presented in Section 2.1.9.3. Comparison of the data from different studies

390   provides some useful insights:

391   • Even though the building height was not a relevant parameter because of the way the experiments

392   were conducted, the full-scale Phalen (1984) data compare reasonably well with 1:10 model scale

393   Kind (1975) data when converted to full-scale.

394   • Kind (1975) 1:10 model-scale data compare reasonably well with Kind (1986) 1:60 model-scale data

395   when converted to full scale for four different gravel sizes without using the correction factor

396   proposed by Kind (1986). However, there is a clear difference between Kind (1975) 1:10 data and

397   Kind (1986) 1:120 data.

398   • Kind (1975) 1:10 model-scale data compare reasonably well with Kopp (2009) 1:20 model-scale data

399   when converted to full scale for two different gravel sizes.

400   These observations suggest that Reynolds number independence can be achieved for specific model

401   scales, whereas Reynolds number effects can be significant and need to be adjusted beyond specific

402	model scales. With these findings, the next section explores the relationship between Froude and

403	Reynolds number.

3. EFFECT OF REYNOLDS NUMBER

405	In the following discussion, the experimental data from Kind's (1975, 1986) 1:10 and 1:60 model-scale

406	experiments are plotted as Fr^2 vs d_* (see Fig. 18) as suggested by Karimpour and Kaye (2012). The plot

407	indicates that the curves are similar for different parapet to building height ratios (H/h), except that they

408	are shifted along the y-axis as the H/h ratio increases. This observation provides confidence that the data

409	can be generalized for a certain class/size of buildings. However, there are no sufficient data to plot

410	similar graphs for high-rise buildings, as well as to ascertain whether very small parapets degrade the

411	performance as observed for roof pavers by Meroney and Bienkiewicz (1986).

412	From Fig. 18, it can be noted that the Froude number is approximately constant with reference to d_*

413	when the non-dimensional diameter (d_*) is greater than 45. This conclusion contradicts the observation

414	made by Karimpour and Kaye (2012), who suggested that, for particle sizes up to $d_* = 75$ for zero

415	parapet height, the Reynolds number is a function of Froude number. The difference between the two

416	studies is that Karimpour and Kaye (2012) experiments (shown by the dashed line in Fig. 18) were

417	conducted for 0^0 wind direction compared to 45^0 in Kind's (1975) studies. Although d_* should only be

418	dependent on the wind shear and not on the wind angle or the building geometry, further research is

419	required in order to explain fully these observed differences.

420	To estimate the physical particle diameter range, the particle diameter can be calculated by rewriting Eq.

421	(1) as (Karimpour and Kaye, 2012)

$$d = \frac{d_*}{\left[\left[\frac{\rho_p - \rho_a}{\rho_a}\right]\frac{g}{v_a^2}\right]^{\frac{1}{3}}} \tag{16}$$

422	where

423	ρ_a = density of air can vary from 1.6 kg/m^3 to 1.09 kg/m^3 for temperatures between -48.15 ^{o}C to
424	 51.85 ^{o}C.

425	ρ_p = density of the particle which is pea gravel or crushed stone can vary between 1500 kg/m^3 when
426	 dry to 2000 kg/m^3 when wet.

427	v_a = Kinematic viscosity of air can vary between 0.935 x 10^{-5} (m^2/s) at -48.15 ^{o}C to 1.807 x 10^{-5}
428	 (m^2/s) at 51.85 ^{o}C.

429	g = acceleration due to gravity is 9.81 m/s^2.

15

430 The calculated particle diameters are summarized in Table 6 for a different range of particle densities. It is
431 noted that, when the particle diameter (d) is greater than approximately 1.3 mm, the Froude number is
432 constant with reference to particle diameter (d) or is independent of Reynolds number. This conclusion
433 suggests that the experimental data from Kind and Wardlaw (1976) can be treated as if the Froude
434 number and the Reynolds number are independent of each other, as the smallest model-scale gravel size
435 that was tested is 2.3 mm which in full scale is 23 mm. This conclusion also implies that extrapolating the
436 data from model scale to full scale using the Froude number is valid for Kind and Wardlaw (1976) data
437 and University of Western Ontario data when corner vortices are the dominant vortical structures that
438 interact with roof aggregate.

4. EXTRAPOLATION LIMITS

440 In general, the experimental data can be extrapolated beyond the range of tested parameters. However,
441 identification of the limits beyond which the extrapolated results may not be representative of the original
442 data set is a challenging task. Therefore, an approach in the following discussion will be used to define
443 these limits so that the recommendations based on the extrapolated data can be used with some
444 confidence. As there is limited data, the extrapolation limits are presented for only two building
445 classifications, i.e., low-rise and high-rise, contrary to four building classification presented in Section
446 2.1.3. The limits for low-rise are presented by combining the data from low-rise and low- to mid-rise
447 buildings and for high-rise are presented by combining the data from high-rise I and high-rise II.

448 In order to define the extrapolation limits, the data from the low- to the mid-rise building are used as the
449 data come from two sources, i.e., from Kind's (1975) and Kopp (2009). There are no other additional data
450 for other building dimensions except Kind (1975). Figure 19 compares the Kind (1975) and Kopp (2009)
451 data by developing the relationships individually. It can be noted that, even though Kind's data are
452 available only up to a parapet height of 1.4 m, when extrapolated they can predict the scouring velocities
453 up to a parapet height of 2.7 m with reasonable accuracy. Hence, it can be stated here that data can be
454 extrapolated up to a parapet height twice what was tested in the experiments for similarly sized buildings.
455 However, this finding, which is based on limited available data, needs to be further justified when
456 additional experimental data become available. Therefore, it is recommended that the extrapolation be
457 conservatively capped at 50 % higher than the maximum parapet height tested by Kind (1975) in his
458 experiments for low- and mid-rise buildings where there is no additional data to support the extrapolation.
459 Accordingly, a parapet height of 2.0 m is recommended as the extrapolation limit for low- and mid-rise
460 buildings.

16

461   For high-rise buildings, only Kind's (1975) data are available from tests up to 0.9 m. As no additional

462   data are available for high-rise buildings similar to low- to mid-rise buildings, it will be assumed here that

463   the 50% higher parapet height value conservatively proposed for low- to mid-rise buildings will also

464   apply, i.e., 1.4 m will be taken as the limit for high-rise buildings. Any recommendations for parapet

465   heights greater than 1.4 m should be treated as having low confidence.

466   Based on the above discussion, Fig. 20 presents a visual representation of the confidence limits for the

467   recommended parapet heights for different building classifications. The top-row plots show the building

468   height (h) or width (w) vs. parapet height ratio (H/h or H/w) for low-/mid-rise or high-rise. The shaded

469   regions indicate the high, medium, and low-confidence regions colored in green, yellow, and white,

470   respectively. The bottom-row plots show the parapet height ratios with building height (H/h) vs. building

471   width (H/w). The shaded regions indicate the envelope of these ratios to qualify them as low-/mid- and

472   high-rise.

5.   LIMITATIONS OF EXISTING DATA

474   There are four main limitations to the data that are reviewed in this paper:

475   • The primary assumption in the whole analysis is that gust wind speeds at the rooftop level that cause

476   failure of roof gravel remain the same for geometrically similar buildings with different heights for

477   any particular gravel size. Even though this assumption appears to be reasonable based on work by

478   Akon (2017), additional experiments are needed to test the effect of the longitudinal turbulence

479   intensity on scouring velocity.

480   • The second limitation of the current data as noted by Kind (1986) and Karimpour and Kaye (2012) is

481   that model-scale experiments carried out in wind tunnels are subject to scaling effects as the

482   requirement of constant Reynolds number cannot be satisfied. Even though it was demonstrated from

483   the Kind's (1975, 1986) data that Reynolds number independence could be achieved after a specific

484   particle diameter for low-rise buildings, this assumption needs to be further investigated for other

485   building sizes. Hence, there is a need to quantify the effect of Reynolds number on the scouring

486   velocity of roof gravel by conducting experiments at different model scales, so that model-scale

487   experiments can be adequately extrapolated to full scale for different building dimensions.

488   • The third limitation of the existing data is that there are no surrounding buildings in the experiments

489   performed by Kind (1975) and the limited number of cases considered at the University of Western

490   Ontario. Therefore, current data could not be directly used to make generalized recommendations.

491   The general trend is that the presence of surrounding buildings can lower the scouring wind speeds

492   based on the findings from the University of Western Ontario experiments. However, it should be

493   noted that this observation is based on experiments on a low-rise building. Generally, surrounding

494   buildings tend to lower the wind speeds on the target building, but the turbulence intensity could be

495   higher compared to that in an open environment. The existing data do not provide a basis to

496   understand the impact of turbulence intensity on critical scouring velocities. Also, the current

497   available experimental data do not tell us the impact of surrounding buildings on target high-rise

498   buildings. Hence, there is a need to explore the effect of surrounding buildings on critical scouring

499   velocity for different building heights.

500 •   The fourth limitation of the existing experimental data is the lack of information to quantify the

501   effects of roof-mounted equipment on the critical scouring velocity of roof gravel. Indeed, there are

502   no data to address this issue. It may be intuitive to assume that roof-mounted equipment will

503   somehow increase the critical scouring velocity and obstruct the gravel from leaving the roof.

504   However, this scenario is less likely as the roof-mounted equipment can produce its own wind field

505   that can interact with the aerodynamics generated by the building (such as separation reattachment

506   flow and corner vortices) and complicate the mechanism that triggers the motion initiation.

507   Additionally, roof-mounted equipment can cause channeling in some cases and sheltering in others.

508   Until some experimental or numerical studies are performed, it is not straightforward to make

509   recommendations as to how roof-mounted equipment will affect the critical scouring velocity of roof

510   gravel.

6. CONCLUSIONS

512 The review paper provides a summary of the different studies for scouring wind speeds of compact roof

513 aggregate. Kind's (1975) data were reanalyzed with the conclusion that the universal gravel size factor

514 proposed by Kind and Wardlaw (1976) based on Froude and Reynolds number independence is not

515 entirely accurate. Accordingly, revised gravel size factors for different classes of buildings are proposed

516 in this paper. These factors when used with Kind's (1986) 1:60 model-scale data along with Froude

517 scaling compare reasonably well with Kind's (1975) 1:10 model-scale data. On the other hand, the

518 comparison with Kind's (1986) 1:120 model-scale data shows that these are substantially different,

519 suggesting that the proposed revised gravel size factors can only partially negate the effect of the Froude

520 and Reynolds number independence assumed by Kind and Wardlaw (1976). A similar conclusion was

521 also reached through the analysis of data from Kind (1985, 1986), namely that the Froude and Reynolds

522 numbers independence can be achieved when the non-dimensional particle diameter $d^* \geq 45$ for low-rise

523 buildings. Even though there is not sufficient information to make a similar conclusion for high-rise

524 buildings, the same is assumed to be valid for the recommendations presented in this paper for all

525 building sizes. Additionally, scouring velocity guidelines are proposed for a new class of buildings, i.e.,

526 low- to mid-rise buildings, by combining the data from Kind (1975) 1:10 model-scale data with Kopp

527 (2009) 1:20 model-scale data. The data analysis demonstrated that the available data can be extrapolated

528 with reasonable confidence up to a parapet height of 2.0 m for low-rise and 1.6 m for high-rise buildings.

529 Extrapolating the available experimental data beyond these parapet heights can be unreliable. The

530 proposed recommendation, even though they are based on available data only up to a building height of

531 45 m, can be used for all building shapes and sizes for any building height as long as they adhere to the

532 non-dimensional building aspect ratios (i.e., l/h or w/h) and parapet height ratios (i.e., H/h or H/w)

533 presented in this study. As a closing, it should be noted that more research is needed to validate the

534 recommendations proposed in this paper to address the limitations of the existing data.

537 **References**

538 Akon, A. F., 2017 Effects of turbulence on the separating-reattaching flow above surface-mounted, three-
539 dimensional bluff bodies. Ph.D. Thesis, University of Western Ontario, London, ON, Canada.

540 Bagnold, R.A., 1937. The transport of sand by wind. The Geographical Journal, 89(5), 409-438.

541 Durst, C.S., 1924. The relationship between current and wind. Quarterly Journal of Royal Metrological
542 Society, 50, 113-119.

543 Holmes, J.D., 2010. Windborne debris and damage risk models: A review. Wind and Structures, 13(2),
544 95-108.

545 Kareem, A., Bashor, R., 2006. Performance of glass/cladding of high-rise buildings in hurricane Katrina.
546 Natural Hazards Modelling Laboratory, University of Notre Dame.

547 Karimpour, A., 2011. An experimental and computational study of windborne debris in severe storms.
548 Ph.D. Thesis, Clemson University, SC, USA.

549 Karimpour, A., Kaye, N.B., 2012. The critical velocity for aggregate blow-off from a built-up roof.
550 Journal of Wind Engineering and Industrial Aerodynamics, 107-108, 83-93.

551 Karimpour, A., Kaye, N.B., 2013. Wind tunnel measurement of the parapet height role on roof gravel
552 blow-off rate for two-dimensional low-rise buildings. Journal of Wind Engineering and Industrial
553 Aerodynamics, 114, 38-47.

554 Kaye, N.B., 2017, Wind-borne debris hazard. ASCE Subcommittee on Wind-Borne Debris, ASCE,
555 Reston, VA, USA.

556 Kind, R.J., 1973. Estimation of critical wind speeds for scouring of gravel or crushed stone on rooftops.
557 National Research Council Canada, Ottawa, Canada, LTR-LA-142.

558 Kind, R.J., 1974. Wind tunnel tests on building models to measure wind speeds at which gravel is blown
559 off rooftops, National Research Council Canada, Ottawa, Canada, LTR-LA-162.

560 Kind, R.J., 1975. Further wind tunnel test on building models to measure wind speed at which gravel is
561 blown off rooftops. National Research Council Canada, Ottawa, Canada, LTR-LA-189.

562 Kind, R.J., Wardlaw, R.L., 1976. Design of rooftops against gravel blow-off. National Research Council
563 of Canada, Ottawa, Canada, Report No. 15544.

564 Kind, R.J., Wardlaw, R.L., 1977. The development of a procedure for the design of rooftops against
565 gravel blow-off and scour in high winds. Proceedings of the Symposium on Roofing Technology, 112-
566 123.

567 Kind, R.J., Savage, M.G., Wardlaw, R.L., 1984. Further model studies of the wind resistance of two
568 loose-laid roof systems (high-rise buildings). National Research Council of Canada, Ottawa, Canada,
569 Report LTR-LA-269.

570 Kind, R.J., Wardlaw, R.L., 1985. Wind tunnel tests on loose-laid roofing systems for flat roofs.
571 Proceedings of the Second International Symposium on Roofing Technology, 230-235.

572 Kind, R.J., 1986. Measurement in small wind tunnels of wind speeds for gravel scour and blow-off from
573 rooftops. Journal of Wind Engineering and Industrial Aerodynamics, 23, 223-235.

574 Kind, R.J., Savage, M.G., Wardlaw, R.L., 1987. Further wind tunnel tests of loose-laid roofing systems,
575 National Research Council of Canada, Ottawa, Canada, Report LTR-LA-294.

576 Kopp, G.A., 2009. A wind tunnel study to observe the characteristics of loose-laid gravel blow-off from a
577 flat roofed low-rise building under wind load, Boundary Layer Wind Tunnel Laboratory Report BLWT-3-
578 2009, University of Western Ontario, London, Canada.

579 Minor, J.E., 1994. Windborne debris and the building envelope. Journal of Wind Engineering and
580 Industrial Aerodynamics, 53, 207-227.

581 Meroney, R.N., Bienkiewicz, B., 1986. Application of wind tunnels to investigations of wind effects on
582 roofs and roof coverings. In: 1986 Spring ASCE Annual Meeting, 7 April 1986, Seattle, WA, USA.

583 Owen, J.S., 2015. Windborne debris in the urban environment. Technical Transactions, 112(2-B), 145-
584 165.

585 Phalen Jr., T.E., 1984. The mechanics of roof gravel instability, scour and movement under wind
586 conditions on single ply loose laid roof membranes. Ideal Concrete Block Company, Waltham, MA.

587 Phalen Jr., T.E., Smith, G.A., 1984. The Properties of commercial stone ballast utilized in the United
588 States on loose-laid single-ply ballasted roof systems. Northeastern University, Boston, MA, Technical
589 Report.

590 Phalen Jr., T.E., 1985. Stone ballast design criteria on loose-laid single-ply ballasted roofs for wind speed,
591 size and weight. Proceedings of the Second International Symposium on Roofing Technology, 236-242.

592 SEAOC-PV2, 2017. Wind design for solar arrays. Structural Engineers Association of California,
593 Sacramento, CA.

594 Shields, A., 1936. Application of similarity principles and turbulence research to bed-load movement. U.
595 S. Department of Agriculture, Soil Conservation Service Cooperative Laboratory, California Institute of
596 Technology, Pasadena, California, Hydrodynamics Laboratory Publ. No 167, W. P. Ott, and J. C. van
597 Uchelen, Transactions.

598 Wills, J.A.B., Lee, B.E., Wyatt, T.A., 2002. A model of windborne debris damage. Journal of Wind
599 Engineering and Industrial Aerodynamics, 80, 555-565.

600 Wu, C.-H., Akon, A.F., Kopp, G.A., 2017. Effects of turbulence on the mean pressure field in the separated-
601 reattaching flow above a low-rise building, Journal of Wind Engineering and Industrial Aerodynamics, 171,
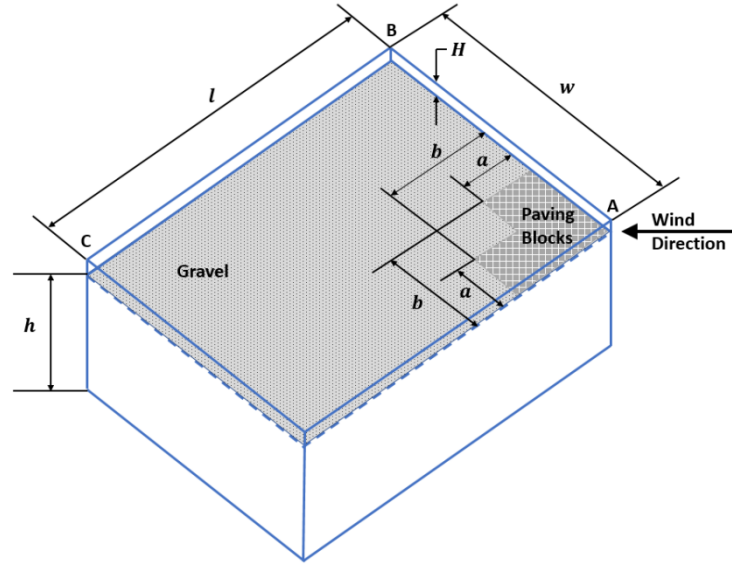602 79-92.

603

Fig. 1.   Definition of different building parameters in Kind's experiments (Kind, 1975). H is the height of the parapet, h is the height of the building, l is the length of the building, w is the width of the building, a is the paver block perpendicular to the edge of the roof, b is the paver block dimension along the edge of the roof, AB is the upstream parapet, and BC is the downstream parapet.
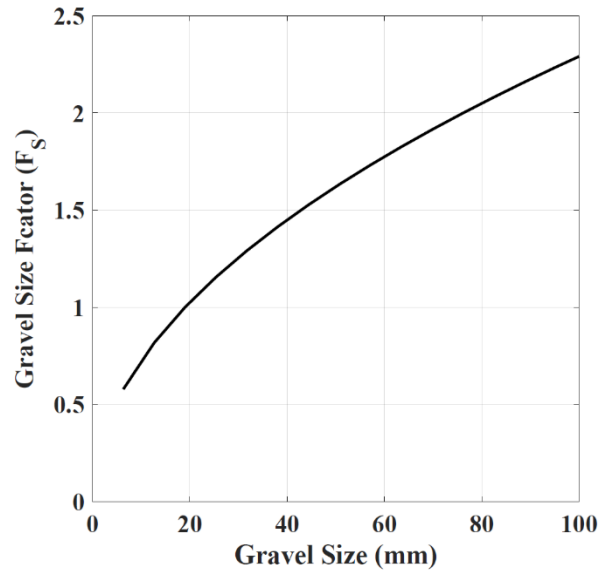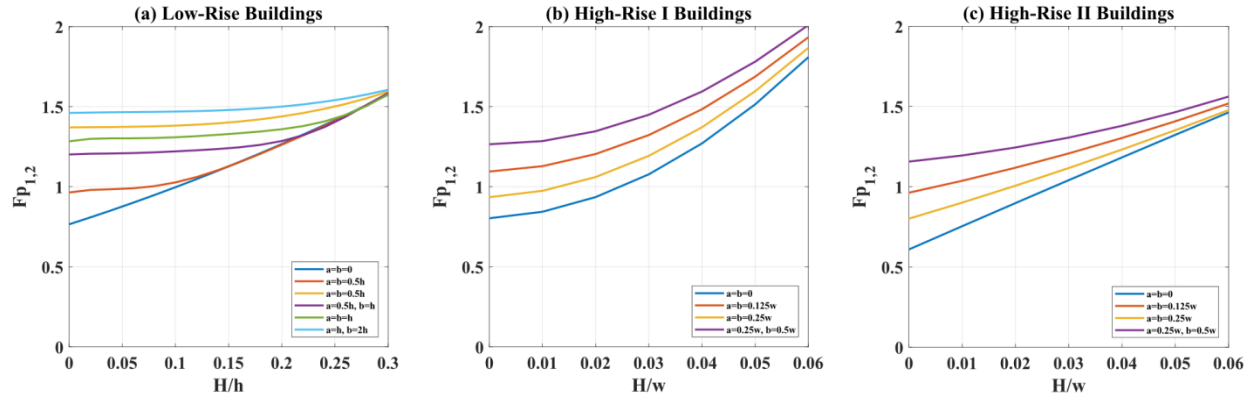
Fig. 2. Gravel size factor.

608

609

610

611 Fig. 3.   Factor (F_P) that accounts for the combined effect of parapet height and paving block arrays on the critical
612   wind speed for U_{c2} applied to (a) low-rise, (b) high-rise I, (c) high-rise II buildings (Kind and Wardlaw,
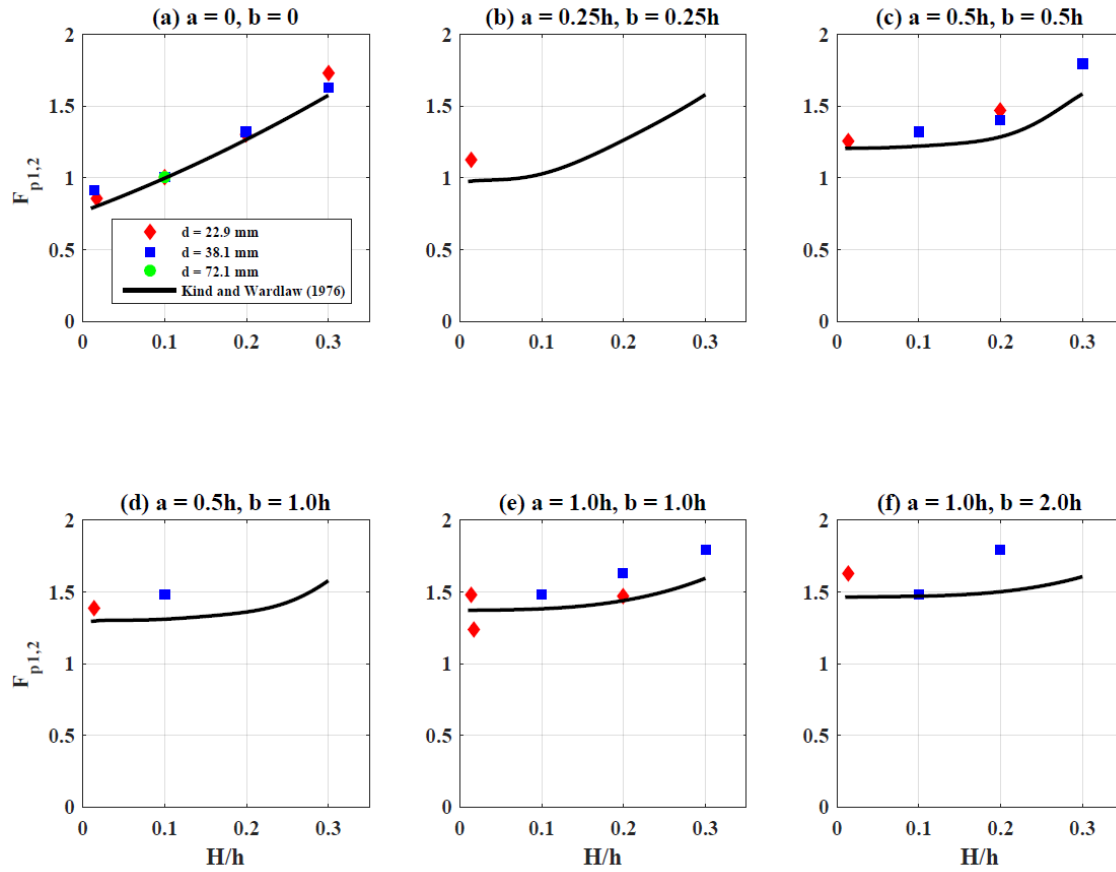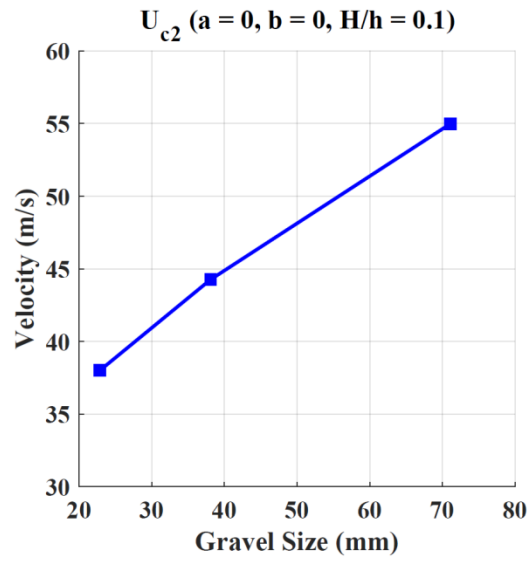613   1976)

614

Fig. 4. Comparison of Factor ($F_{P\,1,2}$) for low-rise building with experimental data from Kind (1975) (see Table 2) for low-rise building divided by critical scouring wind speeds (U_{C2}) at $H/h = 0.1$ for $a = 0$ and $b = 0$ for gravel sizes corresponding to 22.9 mm, 38.1 mm, and 72.1 mm. a and b are the dimensions of the paver blocks, H is the height of the parapet and h is the height of the building.

U_{c_2} (a = 0, b = 0, H/h = 0.1)

621

622   Fig. 5.   Critical velocity for U_{C2} of a low-rise building at $H/h = 0.1$, $a = 0$, and $b = 0$.
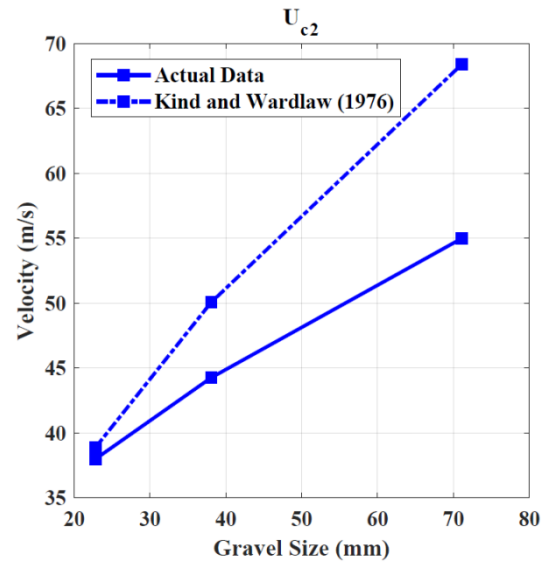
623

Fig. 6.   Comparison of reference velocities from Table 2 with those recommended by Kind and Wardlaw (1976) for a low-rise building.

627

Fig. 7.   Comparison of factor ($F_{P\,1,2}$) for high-rise building I with experimental data from Kind (1975) (see Table 2) divided by critical scouring wind speeds (U_{C2}) at $H/w = 0.025$, $a = 0$ and $b = 0$ for gravel sizes corresponding to 22.9 mm, 38.1 mm, and 72.1 mm. a and b are the dimensions of the paver blocks, H is the height of the parapet and w is the width of the building.

U_{c2}

632

Fig. 8.   Comparison of reference velocities from Table 2 with those recommended by Kind and Wardlaw (1976) for a high-rise building I.

(a) a = 0, b = 0

(b) a = 0.125w, b = 0.125w

(c) a = 0.25w, b = 0.25w
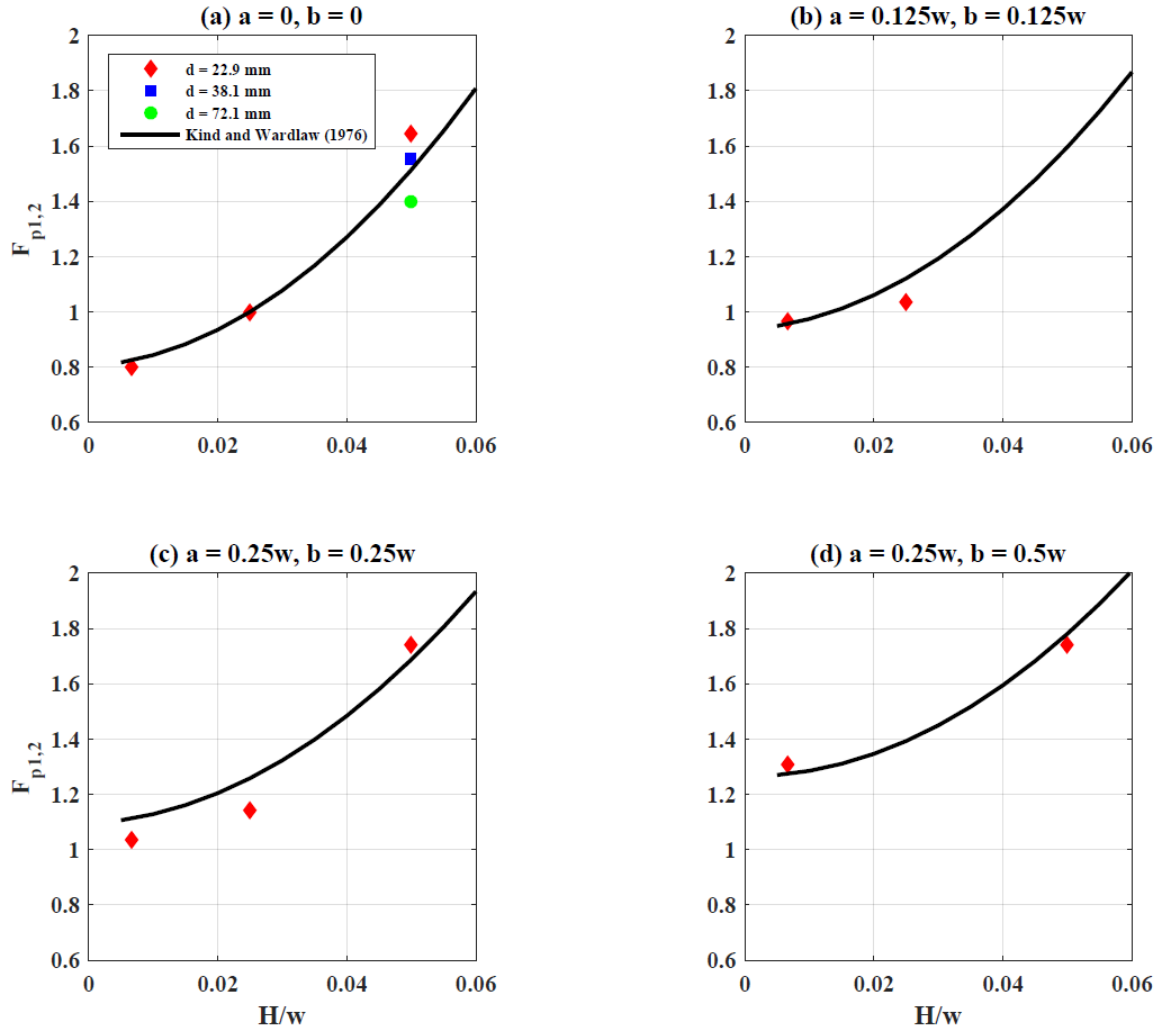
(d) a = 0.25w, b = 0.5w

635

Fig. 9. Comparison of factor ($F_{P\ 1,2}$) for high-rise building II with experimental data from Kind (1975) (see Table 2) divided by critical scouring wind speeds (U_{C2}) at $H/w = 0.025$, $a = 0$ and $b = 0$ for gravel sizes corresponding to 22.9 mm, 38.1 mm, and 72.1 mm. a and b are the dimensions of the paver blocks, H is the height of the parapet and w is the width of the building.
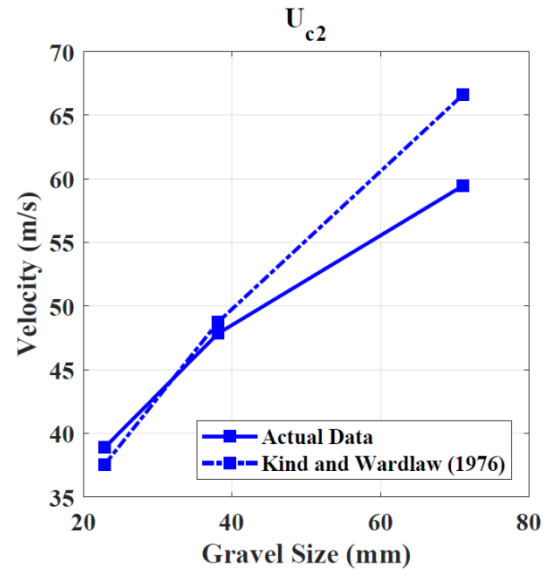
U_c2

640
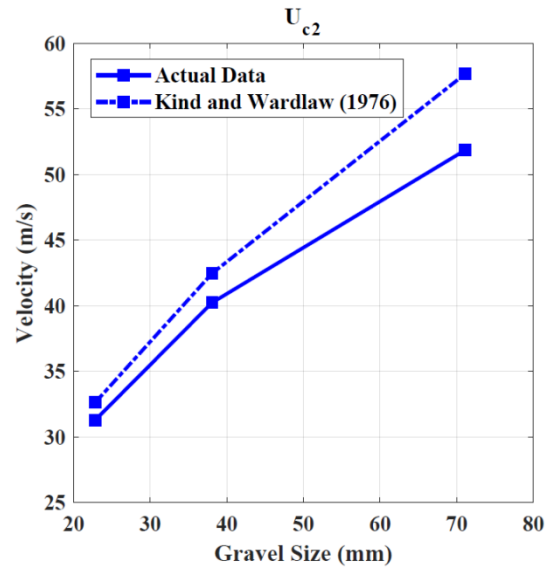
641   Fig. 10.   Comparison of reference velocities from Table 2 with those recommended by Kind and Wardlaw (1976)
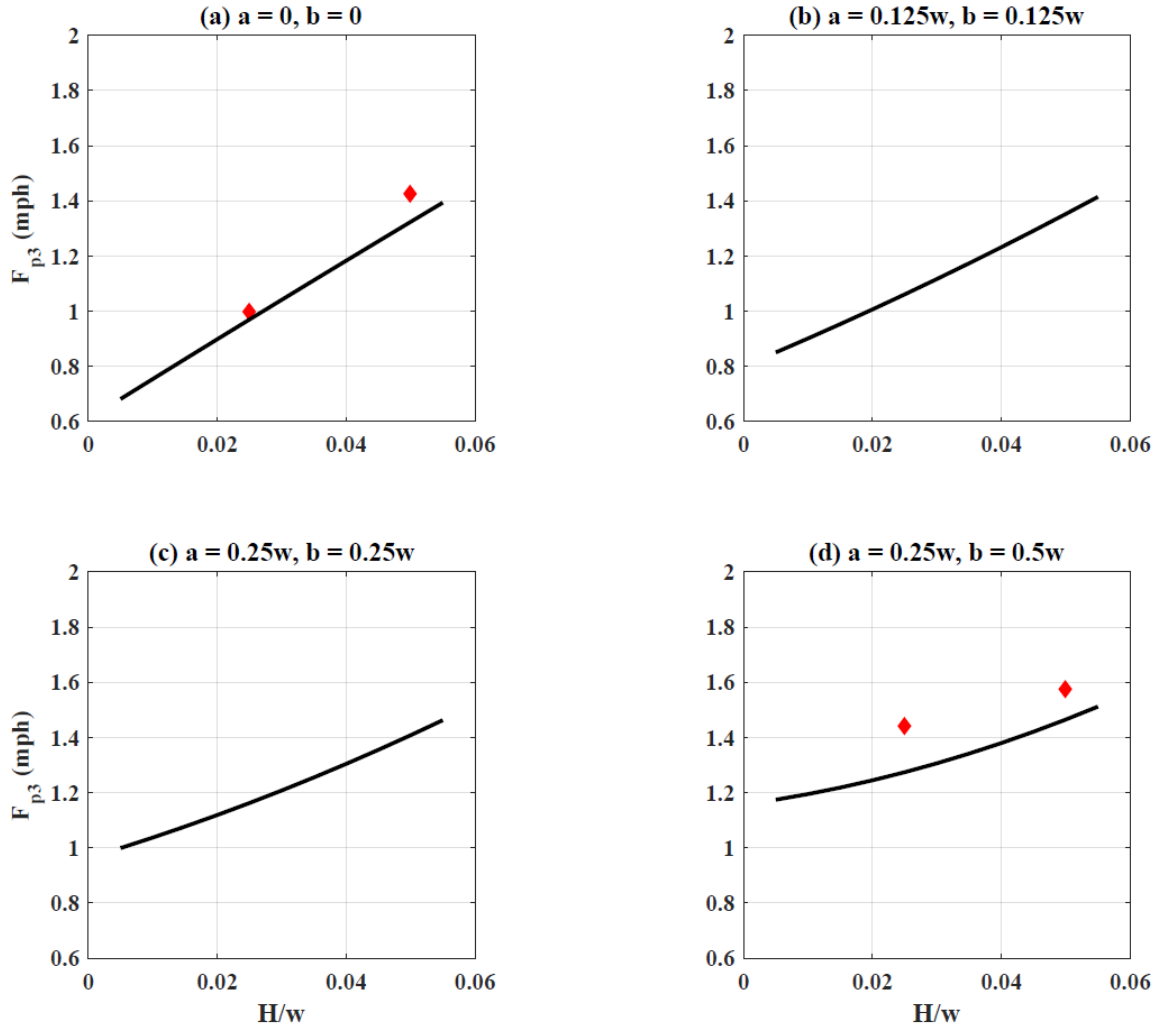642   for a high-rise building II.

643

644

645   Fig. 11.   Velocity correction factor low- and high-rise buildings based on Kind (1975) data.
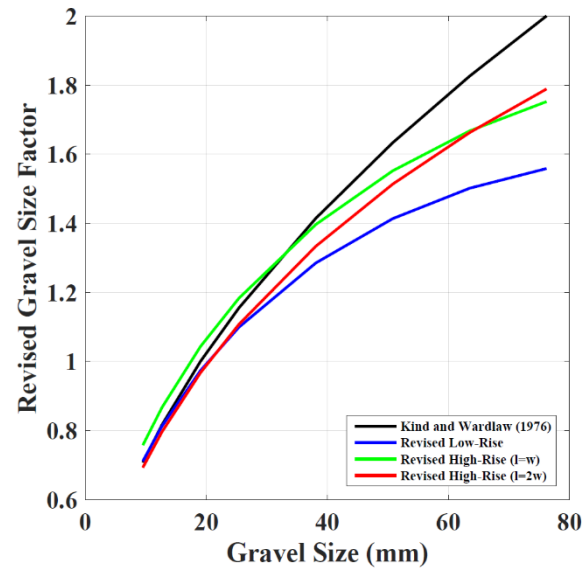
646

647   Fig. 12.   Revised gravel size factor.
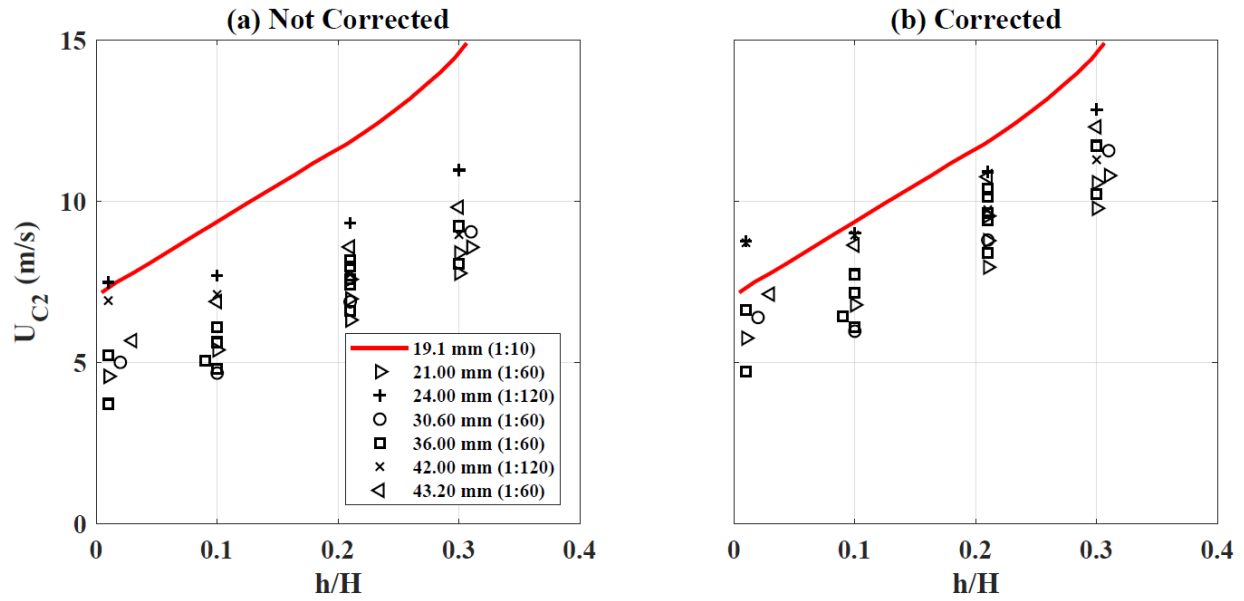
Fig. 13. Comparison of (a) uncorrected and (b) Reynolds number corrected (replotted from Karimpour and Kaye (2012)) model-scale critical scouring wind speeds at roof-height from 1:60 and 1:120 model scale experiments (Kind, 1986) with 1:10 model scale experiments (Kind, 1976) of a low-rise building. The solid line indicates the wind speed from Kind (1975) and the symbols indicate the wind speeds from Kind (1986).

654
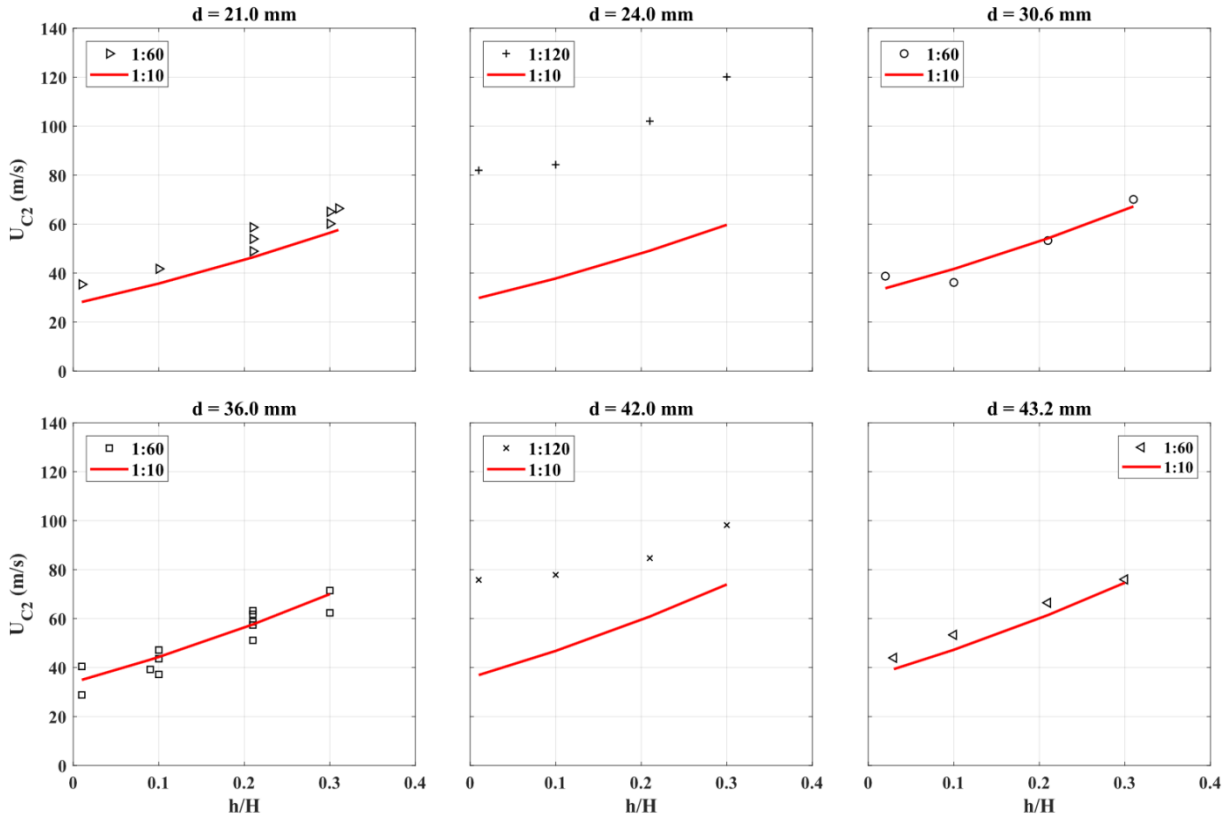
Fig. 14. The ratio of the full-scale critical scouring wind speeds at roof-height from Kind (1986) model scale
experiments with Kind (1976) model scale experiments of a low-rise building (Kind, 1976).

655
656

657

Wind stream

72" Fan Units

Test platform

Observation Platform

658
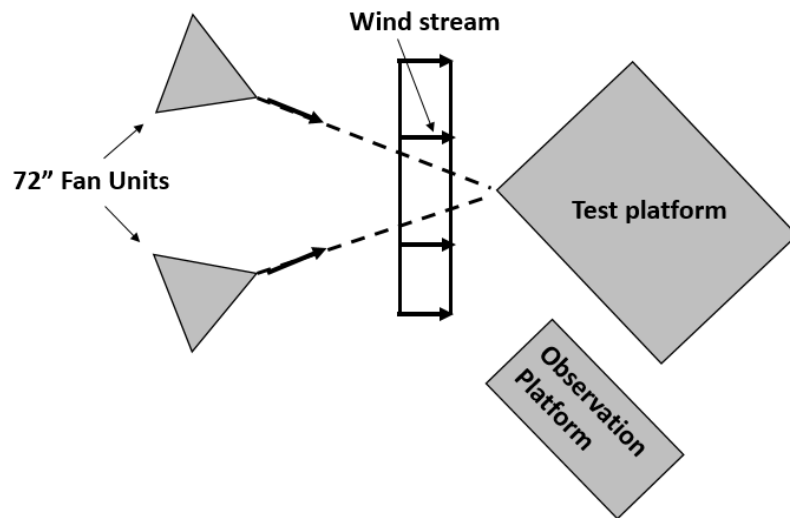
659   Fig. 15.   Experimental setup used by Phalen (1984).

660

661
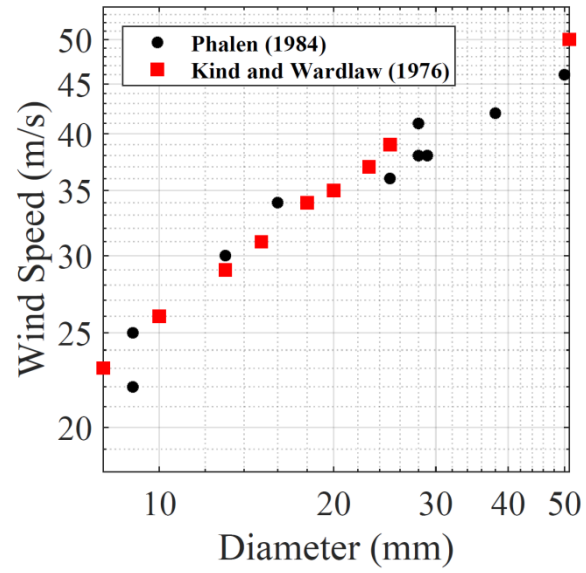
Fig. 16. Comparison of scouring wind speed as a function of stone diameter between Phalen (1984) and Kind and Wardlaw (1976) for the low-rise building with no parapet.

664

665
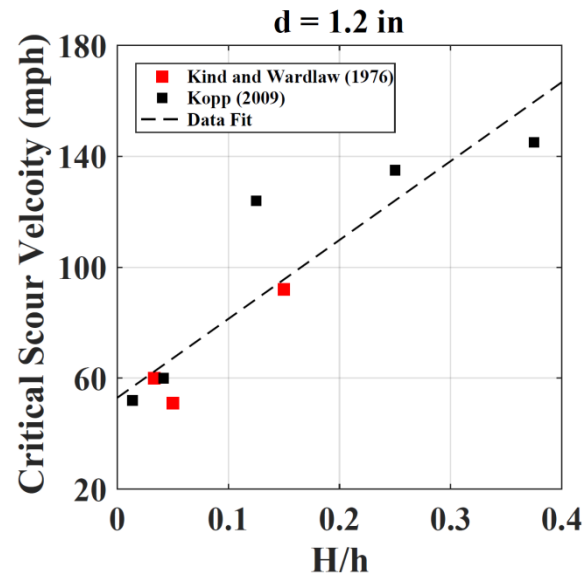
666   Fig. 17.   Comparison of mean hourly critical scouring velocities for the low- to mid-rise building from Kind (1975)
667   and University of Western Ontario that do not conform with Eq.(3).

668
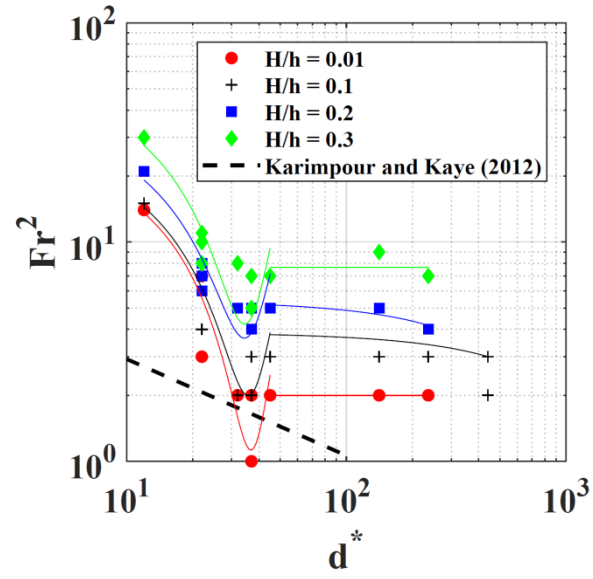
669 Fig. 18. Kind's (1975) critical scouring velocities for low-rise building plotted as Fr^2 vs. d^*. The symbols
670 represent the experimental data and the lines represents the data fit.
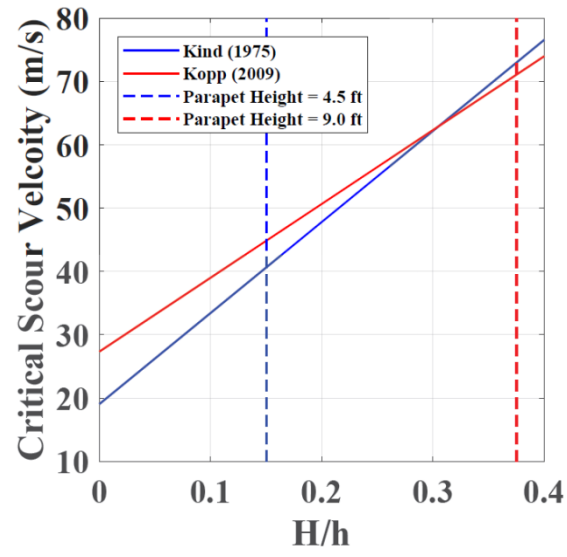
671

672   Fig. 19.   Comparison of Kind's (1975) and Kopp (2009) data for low- to the mid-rise building.
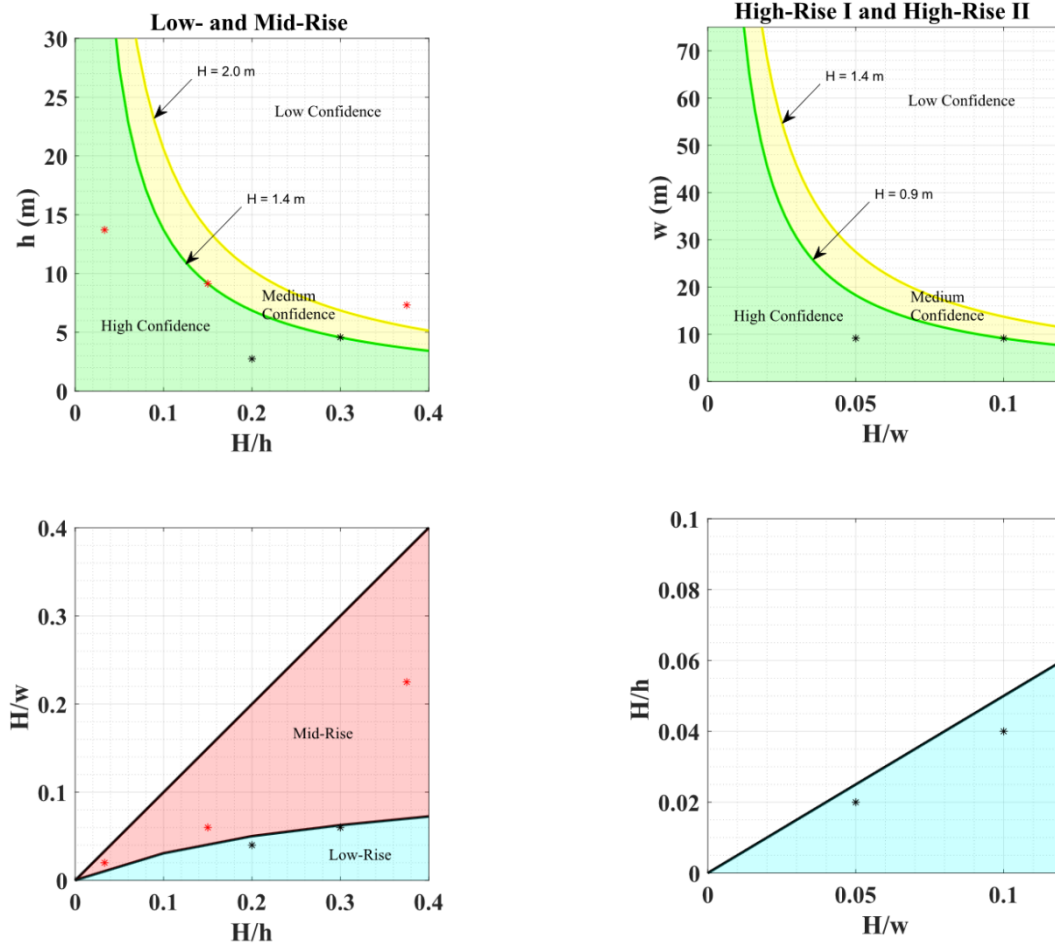
673   Fig. 20.   (Top) Recommendations for confidence in parapet heights for low-, mid- and high-rise buildings.
674   (Bottom) Envelope to qualify the buildings as low-, mid-, and high-rise. The symbols in the plots indicate
675   the experimental data. H is the parapet height, h is the building height, and w is the building width.

676

677   Table 1. Gust factors used to convert mean hourly wind speeds at rooftop level to 1-s gust wind speeds for the data
678   presented in Table 2.

Building Height (m)	Gust Factor
2.74	1.62
4.57	1.6
9.14	1.55
13.72	1.5
22.86	1.2

679

Table 2. Equivalent full-scale data from Kind experiments (Kind, 1975).

Building Height (m)	Building Length (m)	Building Width (m)	Gravel Size (mm)	Parapet Height (m)	Paving Block Array Dimension (a x b) (m)	Wind Direction	U_{C1} (m/s)		U_{C2} (m/s)		U_{C3} (m/s)		U_{C4} (m/s)	
							1 s gust	Mean hourly	1 s gust	Mean hourly	1 s gust	Mean hourly	1 s gust	Mean hourly
4.6	68.6	22.9	38.1	0.06	None	45°	--	--	38.0	23.7	38.0	23.7	68.8	42.9
4.6	22.9	22.9	38.1	0.06	None	45°	27.5	17.0	40.2	25.0	38.0	23.7	55.0	34.4
4.6	22.9	22.9	22.9	0.06	1.14 x 1.14	45°	27.5	17.0	42.9	26.8	38.0	23.7	55.0	34.4
4.6	22.9	22.9	22.9	0.06	2.29 x 2.29	45°	40.2	25.0	47.8	30.0	47.8	30.0	51.9	32.6
4.6	22.9	22.9	22.9	0.06	2.29 x 4.57	45°	46.5	29.1	52.8	33.1	52.8	33.1	58.6	36.7
4.6	22.9	22.9	22.9	0.06	4.57 x 4.57	45°	46.5	29.1	56.3	35.3	55.4	34.9	58.6	36.7
4.6	22.9	22.9	22.9	0.06	4.57 x 9.14	45°	46.5	29.1	61.7	38.5	61.7	38.5	65.3	40.7
4.6	68.6	22.9	38.1	0.46	None	45°	39.3	24.6	50.1	31.3	51.4	32.2	68.4	42.9
4.6	22.9	22.9	22.9	0.46	None	45°	27.3	17.0	38.0	23.7	45.2	28.2	53.6	33.5
4.6	22.9	22.9	38.1	0.46	None	45°	41.6	25.9	51.9	32.6	51.9	32.6	62.6	39.3
4.6	22.9	22.9	38.1	0.46	None	45°	34.4	21.5	44.3	27.7	53.6	33.5	60.8	38.0
4.6	22.9	22.9	71.1	0.46	None	45°	45.2	28.2	55.0	34.4	64.4	40.2	70.2	43.8
4.6	22.9	22.9	38.1	0.46	2.29 x 2.29	45°	48.3	30.4	58.6	36.7	58.6	36.7	65.3	40.7
4.6	68.6	22.9	38.1	0.46	3.05 x 3.05	45°	51.4	32.2	58.6	36.7	68.4	42.9	72.0	45.2
4.6	22.9	22.9	38.1	0.46	2.29 x 4.57	45°	52.8	33.1	65.3	40.7	67.1	42.0	67.1	42.0
4.6	22.9	22.9	38.1	0.46	4.57 x 4.57	45°	52.8	33.1	65.3	40.7	65.3	40.7	65.3	40.7
4.6	22.9	22.9	38.1	0.46	4.57 x 9.14	45°	55.0	34.4	65.3	40.7	71.5	44.7	65.3	40.7
4.6	22.9	22.9	38.1	0.91	None	45°	48.3	30.4	58.6	36.7	64.4	40.2	64.4	40.2
4.6	22.9	22.9	22.9	0.91	2.29 x 2.29	45°	45.2	28.2	55.9	34.9	60.4	37.6	62.1	38.9
4.6	22.9	22.9	38.1	0.91	2.29 x 2.29	45°	58.6	36.7	62.1	38.9	68.0	42.5	72.0	45.2
4.6	22.9	22.9	38.1	0.91	4.57 x 4.57	45°	62.1	38.9	72.0	45.2	76.0	47.4	76.0	47.4
4.6	22.9	22.9	38.1	0.91	4.57 x 9.14	45°	65.3	40.7	79.6	49.6	82.7	51.9	82.7	51.9
4.6	22.9	22.9	22.9	1.37	None	45°	52.8	33.1	65.7	41.1	72.0	45.2	76.0	47.4
4.6	22.9	22.9	38.1	1.37	None	45°	48.3	30.4	72.0	45.2	82.3	51.4	82.3	51.4
4.6	22.9	22.9	38.1	1.37	2.29 x 2.29	45°	55.0	34.4	79.6	49.6	81.8	51.0	81.8	51.0
4.6	22.9	22.9	38.1	1.37	4.57 x 4.57	45°	67.1	42.0	79.6	49.6	82.7	51.9	82.7	51.9
4.6	22.9	22.9	71.1	0.46	None	30°/60°	51.4	32.2	65.3	40.7	72.0	45.2	>84.9	>53.2
4.6	22.9	22.9	38.1	0.46	2.29 x 4.57	30°/60°	48.3	30.4	62.6	39.3	62.6	39.3	69.3	43.4
4.6	22.9	22.9	38.1	0.46	None	90°	65.3	40.7	71.5	44.7	>84.9	>53.2	>84.9	>53.2
2.7	13.7	13.7	22.9	0.05	None	45°	25.9	16.1	32.6	20.1	32.6	20.1	42.5	26.4
2.7	13.7	13.7	22.9	0.05	2.74 x 2.74	45°	39.3	24.1	46.9	29.1	44.7	27.7	49.2	30.4
2.7	13.7	13.7	22.9	0.55	None	45°	40.7	25.0	49.6	30.9	55.4	34.4	59.0	36.2
2.7	13.7	13.7	22.9	0.55	2.74 x 2	45°	46.1	28.6	55.9	34.4	59.0	36.2	59.0	36.2
4.6	22.9	22.9	38.1	0.06	None	45°	72.4	45.2	>84.9	>53.2	>84.9	>53.2	>84.9	>53.2
9.1	22.9	22.9	38.1	0.46	None	45°	34.4	22.4	38.0	24.6	45.6	29.5	51.9	33.5
9.1	22.9	22.9	38.1	1.37	None	45°	49.6	32.2	68.8	44.3	77.8	50.1	77.8	50.1
13.7	22.9	22.9	38.1	0.46	None	45°	34.4	22.8	43.4	29.1	47.4	31.7	56.3	37.6
22.9	9.1	9.1	22.9	0.06	None	45°	24.6	20.6	30.4	25.5	28.2	23.7	34.9	29.1
22.9	9.1	9.1	22.9	0.06	1.14 x 1.14	45°	30.4	25.5	36.7	30.4	39.3	32.6	39.3	32.6
22.9	9.1	9.1	22.9	0.06	2.29 x 2.29	45°	34.9	29.1	39.3	32.6	39.3	32.6	39.3	32.6
22.9	9.1	9.1	22.9	0.06	2.29 x 4.57	45°	39.3	32.6	49.6	41.6	42.0	34.9	42.0	34.9
22.9	9.1	9.1	22.9	0.23	None	45°	30.4	25.5	38.0	31.7	39.3	32.6	39.3	32.6
22.9	9.1	9.1	22.9	0.23	1.14 x 1.14	45°	34.9	29.1	39.3	32.6	39.3	32.6	39.3	32.6
22.9	9.1	9.1	22.9	0.23	2.29 x 2.29	45°	39.3	32.6	43.4	36.2	43.4	36.2	43.4	36.2
22.9	9.1	9.1	22.9	0.46	None	45°	47.8	39.8	62.6	52.3	67.1	55.9	67.1	55.9
22.9	9.1	9.1	38.1	0.46	None	45°	60.8	50.5	74.2	61.7	74.2	61.7	74.2	61.7
22.9	9.1	9.1	71.1	0.46	None	45°	72.0	59.9	>83.2	69.3	--	--	--	--
22.9	9.1	9.1	22.9	0.46	2.29 x 2.29	45°	51.9	43.4	66.2	55.0	69.7	58.1	69.7	58.1
22.9	9.1	9.1	22.9	0.46	2.29 x 4.57	45°	56.3	46.9	66.2	55.0	74.2	61.7	65.3	54.5
22.9	18.3	9.1	22.9	0.23	None	45°	27.7	23.3	30.4	25.5	33.1	27.7	39.3	32.6
22.9	18.3	9.1	22.9	0.23	2.29 x 4.57	45°	33.1	27.7	43.8	36.7	43.8	36.7	43.8	36.7
22.9	18.3	9.1	22.9	0.46	None	45°	34.9	29.1	43.4	36.2	43.4	36.2	43.4	36.2
22.9	18.3	9.1	22.9	0.46	2.29 x 4.57	45°	39.3	32.6	47.8	39.8	47.8	39.8	47.8	39.8
22.9	18.3	9.1	22.9	0.91	None	45°	55.9	46.5	65.3	54.5	65.3	54.5	65.3	54.5
22.9	18.3	9.1	38.1	0.24	None	45°	60.8	50.5	>84.9	>70.6	>84.9	>70.6	>84.9	>70.6

682   Table 3.   Summary of critical scouring velocities from Kind (1986) in model scale.

Model Scale	Parapet Height Ratio (H/h)	Gravel Size (mm)	Mean hourly U_{C2} (m/s)
1:60	0.01	0.35	4.57
	0.1	0.35	5.39
	0.21	0.35	6.97
	0.21	0.35	6.32
	0.21	0.35	7.58
	0.3	0.35	8.40
	0.3	0.35	7.77
	0.31	0.35	8.57
	0.02	0.51	5.00
	0.1	0.51	4.67
	0.21	0.51	6.88
	0.31	0.51	9.05
	0.01	0.6	5.22
	0.01	0.6	3.72
	0.09	0.6	5.06
	0.1	0.6	4.80
	0.1	0.6	6.09
	0.1	0.6	5.63
	0.21	0.6	7.41
	0.21	0.6	6.60
	0.21	0.6	8.17
	0.21	0.6	7.58
	0.21	0.6	7.97
	0.3	0.6	9.23
	0.3	0.6	8.05
	0.03	0.72	5.68
	0.1	0.72	6.89
	0.21	0.72	8.58
	0.3	0.72	9.81
	0.01	0.35	4.57
1:120	0.01	0.2	7.48
	0.1	0.2	7.69
	0.21	0.2	9.32
	0.3	0.2	10.97
	0.01	0.35	6.92
	0.1	0.35	7.11
	0.21	0.35	7.73
	0.3	0.35	8.96

683

684   Table 4.   Summary of critical scouring velocities from Phalen (1984) in full-scale.

Gravel Size (mm)	Mean hourly U_{C2} (m/s)
9.0	22.06
9.4	24.66
12.7	30.13
16.5	33.94
25.1	36.00
28.4	37.69
28.6	38.22
28.2	40.72
38.0	41.55
50.3	45.84
63.5	50.17

685

686   Table 5.   Summary of critical scouring velocities from Kopp (2009) in full-scale.

Building Orientation (deg)	Parapet Height (m)	Gravel Size (mm)	Surrounding Buildings	10 min wind speed at roof height (m/s)
0	0.10	30	No	60.8
	0.30	30	No	60.8
30	0.10	30	No	28.6
	0.30	30	No	28.6
	0.91	30	No	64.4
45	0.10	30	No	25.0
	0.10	30	Yes	32.2
	0.10	43	No	33.5
	0.30	30	No	28.6
	0.30	30	Yes	32.2
	0.30	43	No	35.3
	0.91	30	No	59.5
	1.83	30	No	64.4
	2.74	30	No	69.3

687

688   Table 6.   Summary of calculations for non-dimensional particle diameter for different particle densities.

d^*	ρ_p (kg/m³)	T (ºC)	ρ_a (kg/m³)	υ_a(m²/s)	g (m²/s)	d (mm)
45	1500	-48.15	1.6	0.935×10^{-5}	9.81	0.95
		51.85	1.09	1.807×10^{-5}		1.30
	2000	-48.15	1.6	0.935×10^{-5}		0.87
		51.85	1.09	1.807×10^{-5}		1.18

689

690   Table 7. Equations for Kind and Wardlaw (1976) recommended and revised gravel size factors.

	Low-rise	High-rise ($l = w$)	High-rise ($l = 2w$)
Kind and Wardlaw (1976) recommendation		$F_S = \sqrt{\dfrac{d_p}{(19.1)}}$	
Revised recommendation	$F_S = 0.43\ln{(d_p)} - 0.27$	$F_S = 0.49\ln{(d_p)} - 0.39$	$F_S = 0.53\ln{(d_p)} - 0.57$
Note that the particle diameter (d_p) is in mm.			

691